DOI 10.1007/s11106-021-00215-3
Powder Metallurgy and Metal Ceramics, Vol. 60, Nos. 1-2, May, 2021 (Russian Original Vol. 60, Nos. 1-2, Jan.-Feb., 2021)

REFRACTORY AND CERAMIC MATERIALS

STRUCTURE, STRENGTH, AND OXIDATION RESISTANCE OF ULTRAHIGH-TEMPERATURE ZrB_2–SiC–WC CERAMICS

D.V. Vedel,[1,2] O.N. Grigoriev,[1] P.V. Mazur,[1] and A.E. Osipov[1]

UDC 666.3.7:620.193

The hot pressing process was employed to produce dense ultrahigh-temperature ZrB_2–15 vol.% SiC–5 vol.% WC ceramics. Refractory (Zr, W)C and WB phases emerged in hot pressing at 2050°C and 30 MPa with a holding time of 15 min. The hot pressing process was peculiar in that a (Zr, W)B_2 solid solution formed at the zirconium boride grain boundaries. Annealing in vacuum at 1600°C decreased the amount of oxygen in the ceramics from 0.3 to 0.1 wt.% through interaction of B_2O_3, SiO_2, and ZrO_2 with tungsten carbide. The ZrB_2–15 vol.% SiC–5 vol.% WC ceramics had 505 ± 60 MPa strength at room temperature and 802 ± 94 MPa strength at 1800°C. The high strength at 1800°C was reached through transcrystalline fracture of zirconium boride grains. High-temperature oxidation resulted in scale consisting of three layers: borosilicate glass as the upper layer, zirconium oxide with other oxide phases (WO_3 and SiO_2) as the middle layer, and the base material depleted of boron and silicon as the lower layer. At an oxidation temperature of 1500°C and a holding time of 50 h, the scale was 85 μm thick, including a SiO_2–B_2O_3 layer 64 μm thick and a layer of ZrO_2 + SiO_2 + Me_xO_y and base material depleted of boron and silicon. At an oxidation temperature of 1600°C and a holding time of 2 h, the scale was 84 μm thick, including a SiO_2–B_2O_3 layer 10 μm thick and a layer of ZrO_2 + SiO_2 + Me_xO_y and base material depleted of boron and silicon. The dense scale developed on the material allowed 70% of its initial strength to be retained after oxidation at 1500°C with a holding time of 50 h and 50% strength after oxidation at 1600°C for 2 h, which was higher than for the base ZrB_2–15 vol.% SiC–5 vol.% ceramics.

Keywords: *ultrahigh-temperature ceramics, zirconium diboride, silicon carbide, tungsten boride, oxidation resistance, high-temperature strength.*

INTRODUCTION

Ultrahigh-temperature ceramics (UHTC) produced from borides of transition metals in group IV of the Periodic Table have melting points above 3000°C, high thermal conductivity (>80 W/m · K) [1–3], and excellent corrosion resistance [4–6]. Hafnium boride shows high corrosion resistance but also high specific weight. Possessing

[1]Frantsevich Institute for Problems of Materials Science, National Academy of Sciences of Ukraine, Kyiv, Ukraine.

[2]To whom correspondence should be addressed; e-mail: vedeldv@gmail.com.

Translated from Poroshkova Metallurgiya, Vol. 60, Nos. 1–2 (537), pp. 76–86, 2021. Original article submitted July 29, 2020.

the lowest specific weight, titanium boride exhibits poor oxidation resistance. Zirconium diboride is characterized by an optimal combination of corrosion resistance and specific weight, allowing it to be used as a UHTC matrix. Hence, efforts are ongoing to develop zirconium boride composite ceramics with sintering activators. The activators should not only improve densification but also promote appropriate mechanical properties. Sintering is activated by SiC, Si_3N_4, $MoSi_2$, WC, C, B_4C, $ZrSi_2$, and other additions [7–13].

The ZrB_2–SiC system is a basic zirconium boride ceramic material that shows an optimal combination of mechanical properties. The maximum strength and corrosion resistance are acquired when 15–20 vol.% SiC is added [7–10]. However, silicon carbide is no longer an exhaustive addition: its maximum strength at 1800°C can reach only 200 MPa [11]. The highest strength (836 ± 113 MPa) at 1800°C was exhibited by a ZrB_2–SiC–WC composite [12].

The oxidation resistance of ZrB_2–SiC–WC ceramic composites was studied at 1500°C with a 15-min holding time, the scale being 40 μm thick [13]. The effect of corrosion on the mechanical properties was examined only at 1400°C for the ZrB_2–15 vol.% $MoSi_2$ system [14]. After being held in an oxidizing environment for 100 h, the ceramic composites showed 50% lower strength than the initial value [14].

Our objective is to analyze how phases form in the ZrB_2–15 vol.% SiC–5 vol.% WC system, determine the bending strength of this ceramic composite at room temperature and 1800°C, study its oxidation resistance at 1500°C with a 50 h holding time and at 1600°C with a 2 h holding time, and find out how oxidation influences its bending strength.

EXPERIMENTAL PROCEDURE

The starting powders (Table 1) produced by H.C. Starck (Germany) were mixed in a SAND-1 planetary-ball mill for 5 h in acetone with WC hardmetal grinding balls. The particle size of the ground powder determined by sedimentation was ~0.8–1.5 μm. Then the powder mixture was compacted in steel dies at 100 MPa to reach ~50% of the theoretical density. A combined process was employed to make ceramic composites: annealing in vacuum at 1600°C for 1 h and further hot pressing with an SPD-120 unit at 2050°C, 32 MPa pressure, and isothermal holding for 15 min. The material showed 99% density versus the theoretical value.

The structure of ZrB_2–15 vol.% SiC–5 vol.% WC ceramics was examined by scanning electron microscopy with a Tescan VEGA 3 system with a Bruker detector for electron microprobe analysis and by X-ray diffraction with a DRON-3 diffractometer (Cu-K_α radiation) using a lanthanum hexaboride reference sample. The X-ray diffraction patterns were processed with the NewProfile software.

The samples were oxidized in an LHT 01/17 D furnace (Nabertherm, Germany) in anisothermal conditions in air at 1600°C for 2 h and at 1500°C for 50 h. The samples were cooled down with the furnace.

The samples to be tested by three-point bending at room temperature and 1800°C were 3.5 mm × 4.5 mm × × 36 mm in size. Steel supports with a 20 mm base were used for room-temperature tests and graphite supports for high-temperature tests (1800°C, vacuum).

TABLE 1. Characteristics of the H.C. Starck Starting Powders for Producing ZrB_2–15 vol.% SiC–5 vol.% WC Ceramics

Powder	Grain size d, μm	Admixtures, %	
		O	C
ZrB_2	1	0.5	1
SiC (UF10 grade)	0.74–1	0.6	27.5
WC	0.5–0.7	0.37	6.9

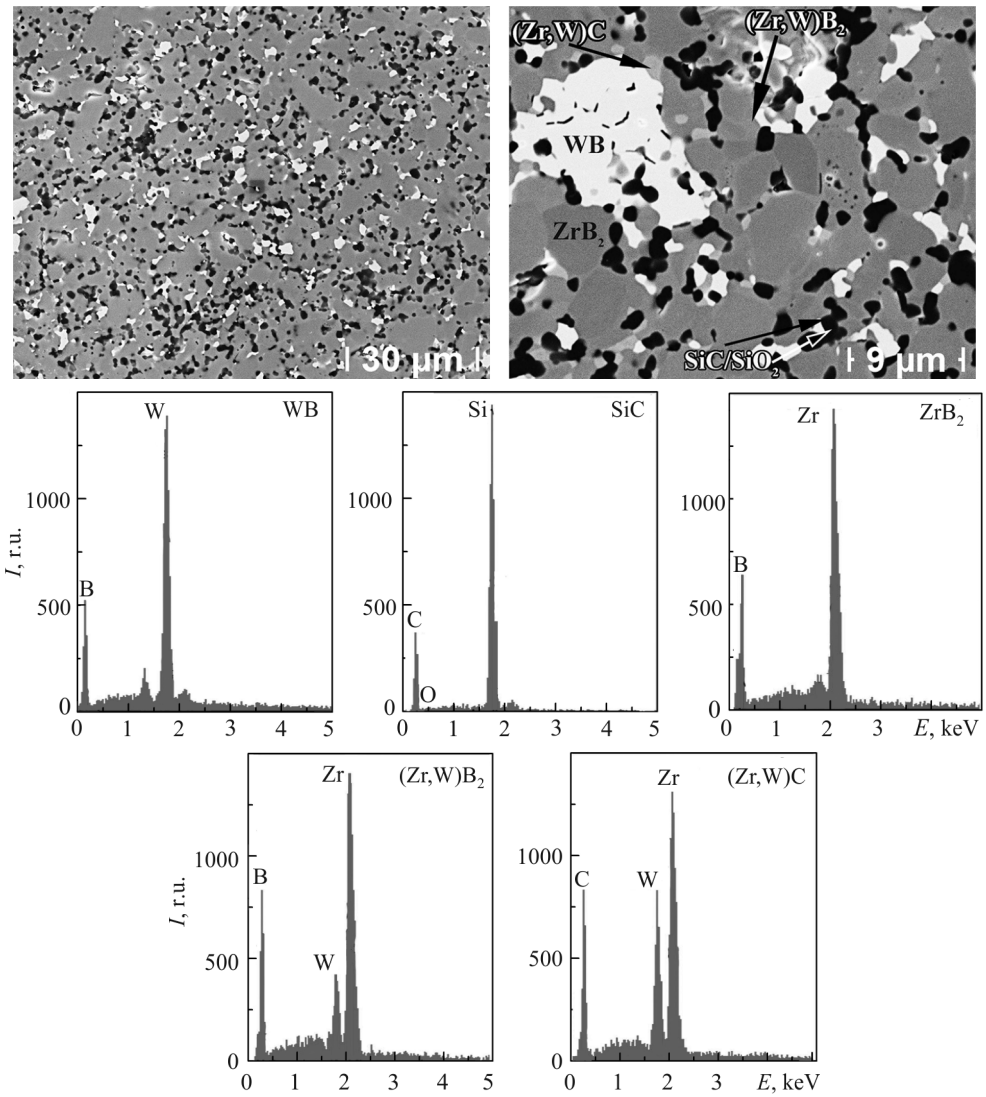

Fig. 1. Microstructure and phase composition of the ZrB_2–15 vol.% SiC–5 vol.% WC ceramic composite

RESULTS AND DISCUSSION

Structurization. Figure 1 shows structure of the material produced. According to microscopic studies, the material contains four phases: gray zirconium diboride, black silicon carbide, light gray zirconium carbide solid solution, and white tungsten boride. The presence of these phases was also ascertained by X-ray diffraction (Fig. 2). The amount of silicon carbide was 14 vol.%, that of zirconium carbide solid solution was 4.4 vol.%, and that of tungsten boride 8.8 vol.%, zirconium diboride being the rest.

As mentioned previously, no components interact to form new phases in the ZrB_2–SiC [11] and SiC–WC [15] systems. Nevertheless, components interact in the ZrB_2–WC [16] and ZrB_2–SiC–WC [17] systems. These systems are common in that zirconium boride solid solutions, zirconium carbide phases, and tungsten boride phases are formed. Interaction of tungsten carbide with oxides present on the starting powder particles is one of the main reactions. The interaction between components can be described by the following reactions:

$$3ZrB_2 + ZrO_2 + 6WC \rightarrow 6WB + 4ZrC + 2CO_{(g)}\uparrow; \quad (1)$$

$$2WC + B_2O_3 \rightarrow 2WB + 3CO_{(g)}\uparrow. \quad (2)$$

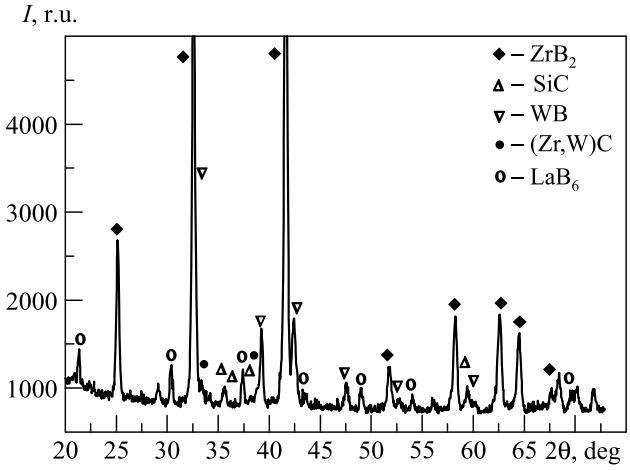

Fig. 2. X-ray diffraction pattern for the hot-pressed ZrB_2–15 vol.% SiC–5 vol.% WC ceramic composite; lanthanum hexaboride used as reference for X-ray diffraction

Oxygen interacts with carbon to form $CO_{(g)}\uparrow$ according to reaction (1). Our calculations indicate that reaction (1) is thermodynamically favored, its free energy at 1900°C being –40 kJ/mole. The likelihood of this reaction to proceed was reported in [12, 13, 15–17].

On the other hand, reaction (2) is more favored than reaction (1) at 1600°C because the Gibbs free energy is –72 kJ/mole. Therefore, annealing at 1600°C in vacuum increases the amount of tungsten boride and decreases the amount of oxygen through interaction between WC and B_2O_3 [13]. Chemical analysis data are also indicative of reduction reactions and oxygen decrease: oxygen amount was 1% in the starting mixture, 0.3% after additional heat treatment, and lower than 0.1% following additional heat treatment and hot pressing. Note also that SiO_2 [21, 22] and B_2O_3 [18] oxides start evaporating above 1100°C in vacuum. Oxygen is concentrated in the SiC phase in the ceramic material in accordance with electron microprobe analysis (Fig. 1).

Zirconium boride solid solutions emerge in the hot pressing process, which is indicated by local microprobe analysis (Fig. 1) and by change in the lattice parameter from 0.3170 nm for pure zirconium boride to 0.3158 nm for its solid solution (Fig. 2). The solubility of tungsten boride in zirconium boride can reach 5 mol.% [19]. The general formula of the solid solution may be $(Zr_{0.97}W_{0.03})B_2$ (Fig. 1). The zirconium diboride solid solution is observed as shells at the grain boundaries and pure zirconium diboride concentrates within the grains (Fig. 1).

Besides the zirconium boride solid solution, a zirconium carbide solid solution is formed. According to [20, 21], the amount of dissolved tungsten in the zirconium carbide phase may exceed 5 mol.%. Hence, zirconium boride and zirconium carbide solid solutions show up when high-temperature ceramic materials are produced. Additional heat treatment in vacuum reduces the amount of oxygen to 0.1%.

TABLE 2. Grain Size and Strength of the Ceramic Composite at Room Temperature and 1800°C

Ceramic composition, vol.%	Grain size, μm					Strength, MPa	
	ZrB_2	(Zr, W)B_2	SiC	WB	(Zr, W)C	Room temperature	1800ºC
ZrB_2–15 SiC–5 WC	–	6.8	5.3	3.8	2.5	505 ± 60	802 ± 94
ZrB_2–5 WC–3 SiC [12]	–	2.5	1.4	2.8	1.2	680 ± 76	836 ± 113
ZrB_2–15 SiC [11]	8	–	2	–	–	500 ± 43	217 ± 17
	4.5	–	2.3	–	–	865 ± 34	112 ± 47

The grain size is among the important factors that determine the mechanical properties. The average grain sizes of the ceramics are summarized in Table 2. The average size of the zirconium boride grains was found considering their shells.

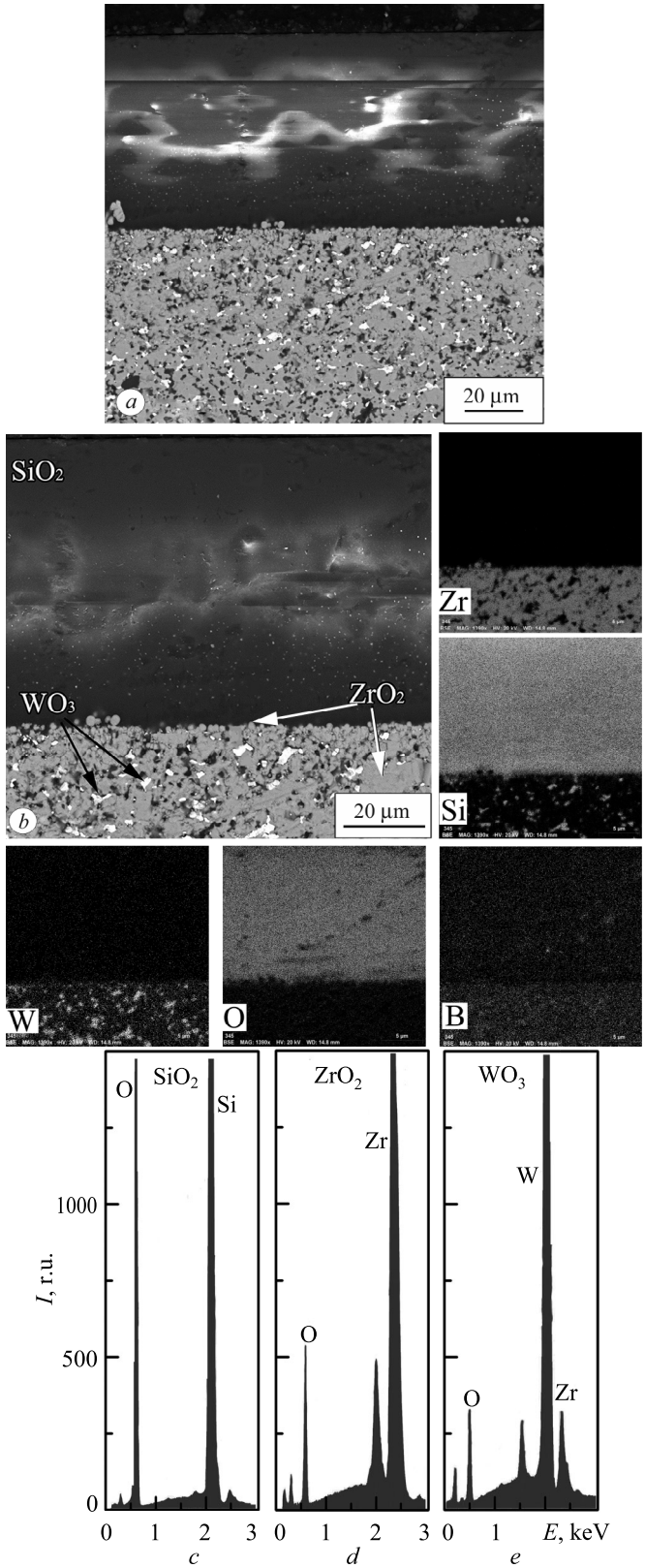

Fig. 3. Cross-sectional microstructure of the ceramic composite oxidized at 1500°C for 50 h: *a*) scale appearance, *b*) upper scale part with distribution of elements; SiO_2 (*c*), ZrO_2 (*d*), and WO_3 (*e*) spectra

Tungsten carbide additions more significantly increase the ceramic strength at 1800°C as rigid grain-boundary phases show up and complicate ductile slipping and fracture at high temperatures. As we reported previously [22] for ZrB_2 UHTC with tungsten-containing additions, grain-boundary shear processes are important for high-temperature tests. In the materials under study, these processes develop at grain boundaries of oxygen-containing SiO_2 phases with low melting points, resulting in microcracks near the boundaries and thus lower strength.

The role of grain-boundary shear processes decreases with smaller areas of grain boundaries (greater grain sizes) and with increasing rigidity of grain-boundary regions, resulting from the presence of grains with solid-solution shells. The solid-solution shells at zirconium boride grain boundaries strengthen the boundary areas of the ceramics. Hence, grain-boundary phases with high melting points prevent grain-boundary shear processes [12, 22]. The emergence of such high-temperature and high-strength phases at grain boundaries allows the ceramics with 800 MPa strength at 1800°C to be produced.

These UHTC structural features are described in [12]. In high-temperature tests of such materials, intercrystalline fracture changes to transcrystalline fracture, including that for grains of other phases (tungsten boride); this increases strain resistance and fracture resistance at 1800°C [23].

A greater amount of tungsten boride increases high-temperature strength [23]. However, the paper [24] indicates that the tungsten-containing component should not exceed 10 vol.% to prevent oxidation resistance from being reduced substantially.

High-Temperature Oxidation. The oxidation of ZrB_2–15 vol.% SiC–5 vol.% WC ceramics is described in [13, 25–27]. However, holding time at 1500°C was no more than 15 min in those studies. This is not sufficient for kinetic processes to occur. The effect of oxidation on residual strength was not considered either.

First consider the material that was oxidized at 1500°C for 50 h. Figure 3*a* shows a cross-section of the oxidized ceramics. The upper scale part consists of SiO_2–B_2O_3 and is 64 μm thick (Fig. 3*a*, *c*). Below is a zirconium oxide layer up to 20 μm thick, with inclusions of tungsten oxide and silicon oxide (Fig. 3*b*, *d*, *e*). The interface between SiO_2–B_2O_3 and $ZrO_2 + Me_xO_y$ is clear and has no cracks or pores (Fig. 3*b*).

We observe somewhat different behavior when oxidation proceeds at 1600°C for 2 h. The cross-section is shown in Fig. 4*a*. The oxidized layer is no more than 85 μm thick, including a SiO_2–B_2O_3 layer 10 μm thick and a $ZrO_2 + SiO_2 + Me_xO_y$ layer. Electron microprobe analysis and X-ray diffraction (Fig. 5) demonstrate that zirconium oxide with inclusions of other phases, such as SiO_2 and WO_3, is the main phase in accordance with the spectra of elements (Fig. 3*c*, *d*).

A clear interface between SiO_2–B_2O_3 and $ZrO_2 + Me_xO_y$ is difficult to see at an oxidation temperature of 1600°C (Fig. 4*a*). This is because liquid SiO_2–B_2O_3 is highly viscous at 1500°C and greater temperatures decease its viscosity, leading to complete spreading on the surface. Since SiO_2–B_2O_3 wets ZrO_2 well, zirconia penetrates between the grains and exerts a splitting effect and we can thus observe individual zirconium dioxide grains in SiO_2–B_2O_3 (Fig. 4*b*).

Therefore, oxidation of the composite is described by reactions (3)–(6). At the initial stage (~800°C), the zirconium boride solid solution oxidizes [5]:

$$ZrB_2 + O_{2(g)} \rightarrow ZrO_2 + B_2O_3; \quad (3)$$

$$WB_2 + 3O_{2(g)} \rightarrow WO_3 + B_2O_3. \quad (4)$$

When temperature increases to 1300°C, silicon carbide oxidizes actively:

$$SiC + O_{2(g)} \rightarrow SiO_2. \quad (5)$$

Holding at 1500°C results in a relatively thick SiO_2–B_2O_3 scale layer (Fig. 3*b*):

$$SiO_2 + B_2O_3 \rightarrow SiO_2–B_2O_3. \quad (6)$$

At an intermediate stage (1000–1200°C), zirconium carbide oxidizes to zirconium oxide and tungsten boride to tungsten oxide.

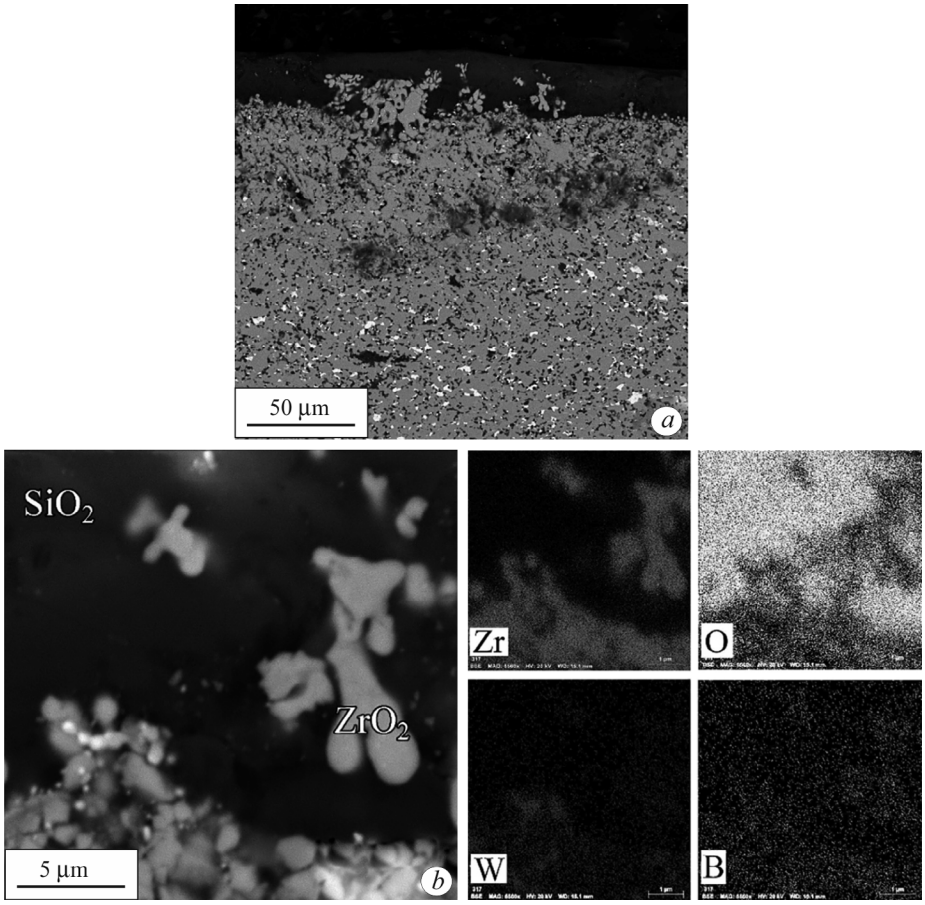

Fig. 4. Cross-sectional microstructure of the ceramic composite oxidized at 1600°C for 2 h: *a*) scale appearance; *b*) upper scale part with distribution of elements

On the other hand, there is a eutectic (1230ºC) in the ZrO_2–WO_3 system [28], allowing the material to be sintered at low temperatures. The paper also reports that tungsten carbide additions improve oxidation resistance of the zirconium boride ceramics through the formation of dense scale layers [29].

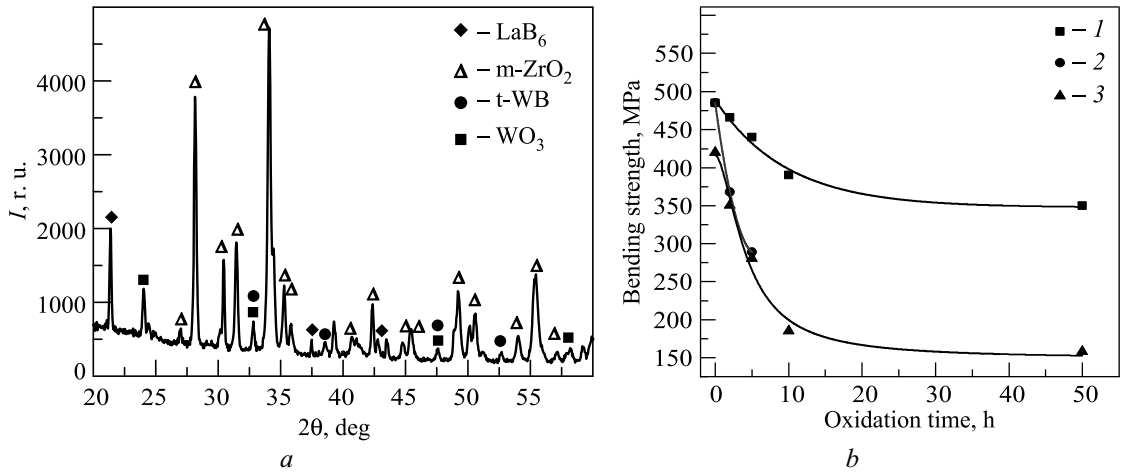

Fig. 5. X-ray diffraction pattern for the ceramic surface oxidized at 1600°C for 2 h against a LaB_6 reference sample *(a)*; bending strength versus oxidation time (*b*) at 1500 (*1*) and 1600°C (*2*) for the ZrB_2–15 vol.% SiC–5 vol.% WC ceramic composite against ZrB_2–15 vol.% SiC after oxidation at 1500°C (*3*)

The residual strength of the UHTC measured after oxidation at 1500°C for 50 h constituted 70% of the initial strength (Fig. 5*b*). The insignificant decrease in strength is due to the development of a dense scale without pores or cracks. Higher oxidation temperature has a more negative effect on the residual strength: it reduces to less than 50% of the initial strength at 1600°C (holding for 2 h). This sharp decrease in strength is due to fracture of the ZrO_2 layer through splitting with the SiO_2–B_2O_3 liquid. Comparison of the ZrB_2–15 vol.% SiC–5 vol.% WC material with the basic ZrB_2–15 vol.% SiC composite indicates that tungsten carbide additions favorably contribute to the residual strength (Fig. 5*b*).

Therefore, a dense three-layer scale develops in the oxidation of ZrB_2–15 vol.% SiC–5 vol.% WC, allowing this material to be reused following oxidation at 1500°C within 50 h and at 1600°C within 2 h.

CONCLUSIONS

Components of the ZrB_2–15 vol.% SiC–5 vol.% WC ceramic composite interact in the hot pressing process to form new phases: WB, (Zr, W)C, and (Zr, W)B_2. These high-temperature and high-strength phases in the (Zr,W)B_2–SiC matrix allow ceramics with 800 MPa strength to be produced at 1800°C.

The scale developed in the oxidation process at 1500 and 1600°C consists of three layers: un upper borosilicate glass layer, a medium layer of zirconium oxide and other oxide phases (WO_3 and SiO_2), and a lower basic material layer depleted of boron and silicon. These layers become thicker with increasing temperature.

The dense scale retains 70% strength of the ceramics after oxidation at 1500ºC (50 h). The residual strength of the ceramics is 50% of the initial strength at an oxidation temperature of 1600°C (2 h).

REFERENCES

1. R. Borrelli, A. Riccio, D. Tescione, R. Gardi, and G. Marino, "Thermo-structural behavior of an UHTC made nose cap of a reentry vehicle," *Acta Astronaut.*, **65**, 442–456 (2009), DOI: https://doi.org/10.1016/j.actaastro.2009.02.016.
2. G.J.K. Harrington and G.E. Hilmas, "Thermal conductivity of ZrB_2 and HfB_2," *Ultra-High Temp. Ceram.: Mater. Extrem. Environ. Appl.*, **9**, 197–235 (2014), DOI: https://doi.org/10.1002/9781118700853.ch9.
3. D.L. McClane, W.G. Fahrenholtz, and G.E. Hilmas, "Thermal properties of (Zr, TM)B_2 solid solutions with TM = Ta, Mo, Re, V, and Cr," *J. Am. Ceram. Soc.*, **98**, 637–644 (2015), DOI: https://doi.org/10.1111/jace.13341.
4. O.N. Grigoriev, I.P. Neshpor, T.V. Mosina, V.B. Vinokurov, A.V. Koroteev, O.V. Buriachek, D.V. Vedel, A.N. Stepanchuk, and L. Silvestroni, "Behavior of ultrahigh-temperature ZrB_2-based ceramics in oxidation," *Powder Metall. Met. Ceram.*, **56**, No. 9–10, 573–580 (2018), DOI: https://doi.org/10.1007/s11106-018-9930-z.
5. L. Silvestroni, G. Meriggi, and D. Sciti, "Oxidation behavior of ZrB_2 composites doped with various transition metal silicides," *Corros. Sci.*, **83**, 281–291 (2014), DOI: https://doi.org/10.1016/j.corsci.2014.02.026.
6. L. Silvestroni, S. Failla, I. Neshpor, and O. Grigoriev, "Method to improve the oxidation resistance of ZrB_2-based ceramics for reusable space systems," *J. Eur. Ceram. Soc.*, **38**, 2467–2476 (2018), DOI: https://doi.org/10.1016/j.jeurceramsoc.2018.01.025.
7. W. Li, Y. Zhang, X. Zhang, C. Hong, and W. Han, "Thermal shock behavior of ZrB_2–SiC ultra-high temperature ceramics with addition of zirconia," *J. Alloys Compd.*, **478**, 386–391 (2019), DOI: https://doi.org/10.1016/j.jallcom.2008.11.045.
8. P.V. Mazur, O.N. Grigoriev, D.V. Vedel, and L.M. Melakh, "Properties of ZrB_2–SiC–CrB_2 ceramics produced by vacuum sintering," *Elektron. Mikrosk. Mitsn. Mater.*, No. 25, 43–54 (2019), DOI: http://www.materials.kiev.ua/publications/ EMMM/2019/11.pdf.
9. Y.H. Seong and D.K. Kim, "Oxidation behavior of ZrB_2–*x*SiC composites at 1500°C under different oxygen partial pressures," *Ceram. Int.*, **40**, 15303–15311 (2014), DOI: https://doi.org/10.1016/j.ceramint.2014.07.036.
10. W.B. Han, P. Hu, X.H. Zhang, J.C. Han, and S.H. Meng, "High-temperature oxidation at 1900°C of ZrB_2–*x*SiC ultrahigh-temperature ceramic composites," *J. Am. Ceram. Soc.*, **91**, 3328–3334 (2008), DOI: https://doi.org/10.1111/j.1551-2916.2008.02660.x.

11. P. Hu and Z. Wang, "Flexural strength and fracture behavior of ZrB_2−SiC ultra-high temperature ceramic composites at 1800°C," *J. Eur. Ceram. Soc*., **30**, 1021–1026 (2010), DOI: https://doi.org/10.1016/j.jeurceramsoc.2009.09.029.
12. L. Silvestroni, H.J. Kleebe, W.G. Fahrenholtz, and J. Watts, "Super-strong materials for temperatures exceeding 2000°C," *Sci. Rep*., **7**, 1–8 (2017), DOI: https://doi.org/ 10.1038/srep40730.
13. F. Monteverde and L. Silvestroni, "Combined effects of WC and SiC on densification and thermo-mechanical stability of ZrB_2 ceramics," *Mater. Des.*, **109**, 396–407 (2016), https://doi.org/10.1016/j.matdes.2016.06.114.
14. D. Sciti, M. Brach, and A. Bellosi, "Long-term oxidation behavior and mechanical strength degradation of a pressurelessly sintered ZrB_2–$MoSi_2$ ceramic," *Scr. Mater*., **53**, 1297–1302 (2005), DOI: https://doi.org/10.1016/j.scriptamat.2005.07.026.
15. J. Zou, G.J. Zhang, S.K. Sun, H.T. Liu, Y.M. Kan, J.X. Liu, and C.M. Xu, "ZrO_2 removing reactions of groups IV–VI transition metal carbides in ZrB_2 based composites," *J. Eur. Ceram. Soc*., **31**, 421–427 (2011), DOI: https://doi.org/10.1016/ j.jeurceramsoc.2010.10.011.
16. H. Bin Ma, G.J. Zhang, H.L. Liu, J.X. Liu, Y. Lu, and F.F. Xu, "Effect of WC or ZrC addition on thermal residual stresses in ZrB_2–SiC ceramics," *Mater. Des*., **110**, 340–345 (2016), DOI: https://doi.org/10.1016/j.matdes.2016.08.009.
17. J. Zou, G.J. Zhang, C.F. Hu, T. Nishimura, Y. Sakka, J. Vleugels, and O. Van Der Biest, "Strong ZrB_2–SiC–WC ceramics at 1600°C," *J. Am. Ceram. Soc*., **95**, 874–878 (2012), DOI: https://doi.org/10.1111/j.1551-2916.2011.05062.x.
18. V. Korobtsov, V. Balashev, and K. Bazarsad, "B_2O_3 decomposition on the Si (100) surface," *Phys. Low-Dimens. Struct*., **2**, 34–41 (2006).
19. B. Post, F.W. Glaser, and D. Moskowitz, "Transition metal diborides," *Acta Metall*., **2**, 20–25 (1954), DOI: https://doi.org/10.1016/0001-6160(54)90090-5.
20. I.L. Shabalin, *Ultra-High Temperature Materials I. Carbon (Graphene/Graphite) and Refractory Metals*, Springer Dordrecht Heidelberg, New York, London (2014), DOI: https://doi.org/10.1007/978-94-007-7587-9.
21. Yu.B. Kuz'ma, T.F. Fedorov, and E.A. Shvets, "Phase equilibria in the system Zr–W–C," *Powder Metall. Met. Ceram.*, **4**, No. 2, 106–109 (1965), DOI: https://doi.org/10.1007/BF00777011.
22. L. Silvestroni, S. Failla, V. Vinokurov, I. Neshpor, and O. Grigoriev, "Core–shell structure: An effective feature for strengthening ZrB_2 ceramics," *Scr. Mater*., **160**, 1–4 (2019), DOI: https://doi.org/10.1016/j.scriptamat.2018.09.024.
23. L. Silvestroni, N. Gilli, A. Migliori, D. Sciti, J. Watts, G.E. Hilmas, and W.G. Fahrenholtz, "A simple route to fabricate strong boride hierarchical composites for use at ultra-high temperature," *Compos. Part B Eng*., **183**, 1–22 (2020), DOI: https://doi.org/10.1016/j.compositesb.2019.107618.
24. S.C. Zhang, G.E. Hilmas, and W.G. Fahrenholtz, "Oxidation of zirconium diboride with tungsten carbide additions," *J. Am. Ceram. Soc*., **94**, 1198–1205 (2011), DOI: https://doi.org/10.1111/j.1551-2916.2010.04216.x.
25. J. Zou, V. Rubio, and J. Binner, "Thermoablative resistance of ZrB_2–SiC–WC ceramics at 2400°C," *Acta Mater*., **133**, 293–302 (2017), DOI: https://doi.org/10.1016/j.actamat.2017.05.033.
26. L. Silvestroni, D. Sciti, F. Monteverde, K. Stricker, and H.J. Kleebe, "Microstructure evolution of a W-doped ZrB_2 ceramic upon high-temperature oxidation," *J. Am. Ceram. Soc*., **100**, No. 4, 1760–1772 (2017), DOI: https://doi.org/10.1111/jace.14738.
27. A.L. Chamberlain, W.G. Fahrenholtz, G.E. Hilmas, and D.T. Ellerby, "High-strength zirconium diboride-based ceramics," *J. Am. Ceram. Soc*., **87**, 1170–1172 (2004), DOI: https://doi.org/10.1111/j.1551-2916.2004.01170.x.
28. G.R. Kowach, "Growth of single crystals of $Zr_2W_2O_8$," *J. Cryst. Growth*, **212**, 167–172 (2000), DOI: https://10.1016/j.jcrysgro.2011.12.081.
29. A.L. Chamberlain, W.G. Fahrenholtz, and G.E. Hilmas, "Pressureless sintering of zirconium diboride," *J. Am. Ceram. Soc*., **89**, 450–456 (2006), DOI: https://doi.org/10.1111/ j.1551-2916.2005.00739.x.